scientific **data**

Check for updates

OPEN

DATA DESCRIPTOR

A bite force database of 654 insect species

Peter Thomas Rühr[ORCID][1,2 ✉], Carina Edel[1], Melina Frenzel[1] & Alexander Blanke[1]

Bite force is a decisive performance trait in animals because it plays a role for numerous life history components such as food consumption, inter- and intraspecific interactions, and reproductive success. Bite force has been studied across a wide range of vertebrate species, but only for 32 species of insects, the most speciose animal lineage. Here we present the insect bite force database with bite force measurements for 654 insect species covering 476 genera, 111 families, and 13 orders with body lengths ranging from 3.76 to 180.12 mm. In total we recorded 1906 bite force series from 1290 specimens, and, in addition, present basal head, body, and wing metrics. As such, the database will facilitate a wide range of studies on the characteristics, predictors, and macroevolution of bite force in the largest clade of the animal kingdom and may serve as a basis to further our understanding of macroevolutionary processes in relation to bite force across all biting metazoans.

Background & Summary

Bite force is a performance trait which may decide on an animal's ability to acquire food, win inter- and intra-specific fights, and successfully reproduce[1–5]. In vertebrates, maximum bite forces are well studied across a wide diversity of taxa such as bony fishes[6,7], crocodilians (e.g.[8]), birds (e.g.[9]), turtles (e.g.[10]), squamates (e.g.[11,12]), frogs[13], marsupials[14], and mammals (e.g.[15–18]). Fundamental knowledge on the variation, predictors, and evolution of bite forces within the omnipresent insects is, however, lacking. Even though more than half a million insect species belong to orders that possess biting-chewing mouthparts[19,20], existing literature only yields maximum bite force measurements on five dragonflies[21,22], one cockroach[23], 12 ants[24–27], and 14 beetles[28,29]. This is despite the fact that biting-chewing insects include the most destructive plant-feeding animals and occupy crucial roles in the world's ecosystems as soil-building detritivores[30].

So far, measuring bite forces of insects was hampered by their small size, but the recently published measurement setup "forceX"[31] overcame this limitation to some extent by allowing minimally invasive *in vivo* bite force measurements of animals with gape sizes more than ten times smaller than previous setups (e.g.[32]). Using forceX, we measured bite forces of 654 insect species from 111 families in 13 orders, collected on four continents and from numerous breeding cultures. Instead of gathering maximum force values only, as most previous bite force studies have done (but see[21–23,29,33]), we also recorded force curves. In addition, the bite force database contains head, thorax, wing, and body metrics of each specimen to assess morphological predictors for bite force in insects. Thus, the database will facilitate investigations on the macroevolution of maximum bite forces, bite lengths, bite frequencies, muscle activation patterns, and bite curve shapes across the megadiverse insects and will facilitate comparisons with all biting metazoan taxa.

Methods

Collection and material.
A total of 1906 bite force series from 1290 insect specimens representing 654 species in 476 genera in 194 subfamilies, 111 families, and 13 orders were collected in Australia, China, Denmark, France, Germany, Greece, Panama, and Slovenia using light traps, insect nets, pitfall traps, or directly by hand. All specimens were collected under the respective regulations in effect (see Acknowledgements). Additionally, we measured specimens from numerous scientific, private, and commercial insect breeders and traders (Supplementary Table 1 and Acknowledgements).

Size measurements.
Head width, head length, head height, thorax width, forewing length, and body length measurements were performed to the nearest 0.01 mm using a digital caliper (77001, Wentronic GmbH, Braunschweig, Germany). For the head width, the longest distance from left to right was measured, including

[1]Bonn Institute for Organismic Biology (BIOB), Section 2: Animal Biodiversity, University of Bonn, An der Immenburg 1, 53121, Bonn, Germany. [2]Institute of Zoology, University of Cologne, Zülpicher Str. 47b, Cologne, 50674, Germany. ✉e-mail: pruehr@evolution.uni-bonn.de
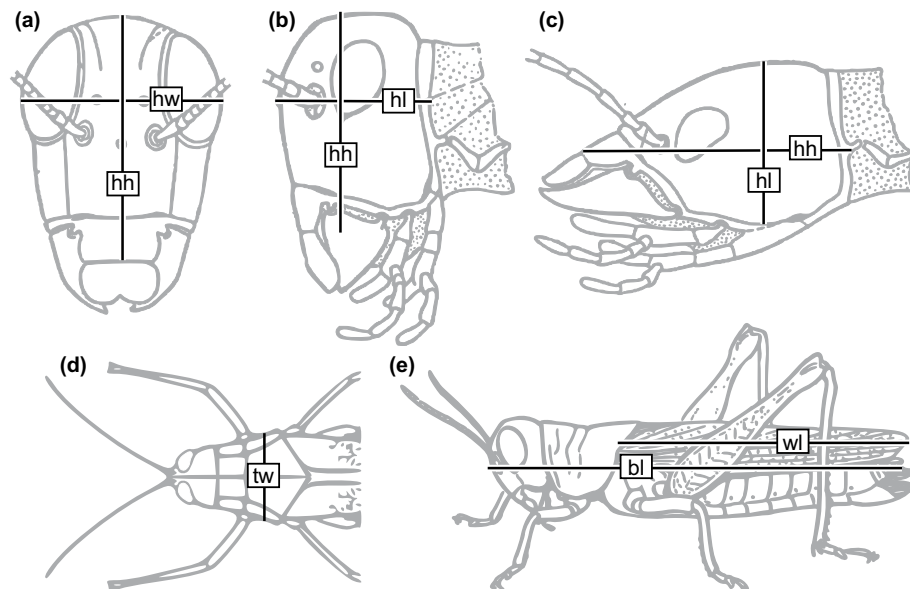
Fig. 1 Insect length measurements. (**a,b**) Head of an orthognathous insect in frontal (**a**) and lateral view (**b**). (**c**) Head of a prognathous insect in lateral view. (**d**) Frontal part of an orthognathous insect in dorsal view. (**e**) Habitus of an orthognathous insect in lateral view. Abbreviations: **bl**: body length; **hh**: head height; **hl**: head length; **hw**: head width; **tw**: thorax width; **wl**: forewing length. a,b,c after Snodgrass[50]; d after own photo, e after Snodgrass[51]. Figures not to scale.

protruding eyes if applicable (Fig. 1a). Head height in orthognathous insects was measured from the clypeo-labral suture to the dorsal end of the head (Fig. 1a,b). In prognathous insects, head length was measured from the clypeo-labral suture to the posterior end of the head (Fig. 1c). Thorax width was measured on the prothorax (Fig. 1d) and excluded lateral protrusions as found e.g. in many cockroaches and praying mantises. Body length measurements excluded cerci, ovipositors, or other abdominal appendages (Fig. 1e).

Bite force measurements. All measurements were carried out with the metal-turned version of the forceX setup as described in[31]. In short, live and conscious animals were held between two fingers, rotated by 90° along their body axis and allowed to voluntarily bite on the tip elements of the forceX. Different tip element designs[31] and distances between them were used to accommodate different animal gape sizes. During measurements, animals were observed through the Junior Stereo 3D microscope (Bresser GmbH, Rhede, Germany) that is part of the forceX setup to ensure that gape sizes are suitable and that the insects bite at the edge of the tip elements so that the ratio of the forceX lever remains at a constant 0.538[31,34]. We also checked if the animals bit with the distal-most incisivi of their mandibles to ensure that measurements remain comparable[31,34]. Non-distal bites or wrongly placed bites on the tip elements were discarded. If animals did not start biting by themselves, we used the tip element protrusions to insert the tip elements between the mandibles and/or used a fine brush to touch the animal's cerci, head or abdomen[23]. Amplified analogue voltage signals were converted to a digital signal by a 12-bit USB data acquisition device (U3-HV, LabJack Corporation, Lakewood, Colorado, US) and recorded with the LJStreamUD v1.19 measurement software (LabJack Corporation) on a computer.

Data curation. Subsequent data curation was performed in the software environment 'R' v. 4.2.2[35] using the package 'forceR' v.1.0.20[31]. Since the forceR package was written to analyse data generated with the forceX setup, we used, if not stated otherwise, the default settings of the package functions. After initial download of the raw data from Zenodo *via* zen4R v.0.8[36], time series were converted from the output format of LJStreamUD to a *.csv file containing only a time and a voltage column (without changing measurement values) using the forceR function 'convert_measurement()'. Then, all measurements were manually cropped using 'crop_measurement()' to exclude regions without bite data at the beginning and end of each measurement. Next, 'amp_drift_corr()' was used to correct for the logarithmic drift of the analogue charge amplifier (see[31] for details). When using the high amplification setting (20 V/N) to amplify the miniscule voltage signals of the piezoelectric force transducer at small bite forces, the zero-voltage-line ('baseline') may drift notably during a measurement. Therefore, a PDF file depicting all input raw data and their amplifier drift-corrected data graphs (available at Zenodo, s. Data Records) was visually inspected, and, if necessary, the function 'baseline_corr()' was used in its automatic mode to correct for this drift. In some of these cases, however, especially when the test animals showed long, plateau-like bite curve shapes, the automatic mode of 'baseline_corr()' failed to find the baseline, and the manual mode was used. All corrections can be retraced in the PDF file and reproduced using the log files that were created during corrections and which are stored at Zenodo. With the function 'reduce_frq()' we then reduced the sampling rate of all time series to 200 Hz, a value found to be sufficient to represent insect bite force curves[21–23,29] to reduce the amount of data for further analyses. As a last curating step, voltage values were converted into force data [N] with the forceR function 'y_to_force()' that considers the amplification level of each measurement and the lever
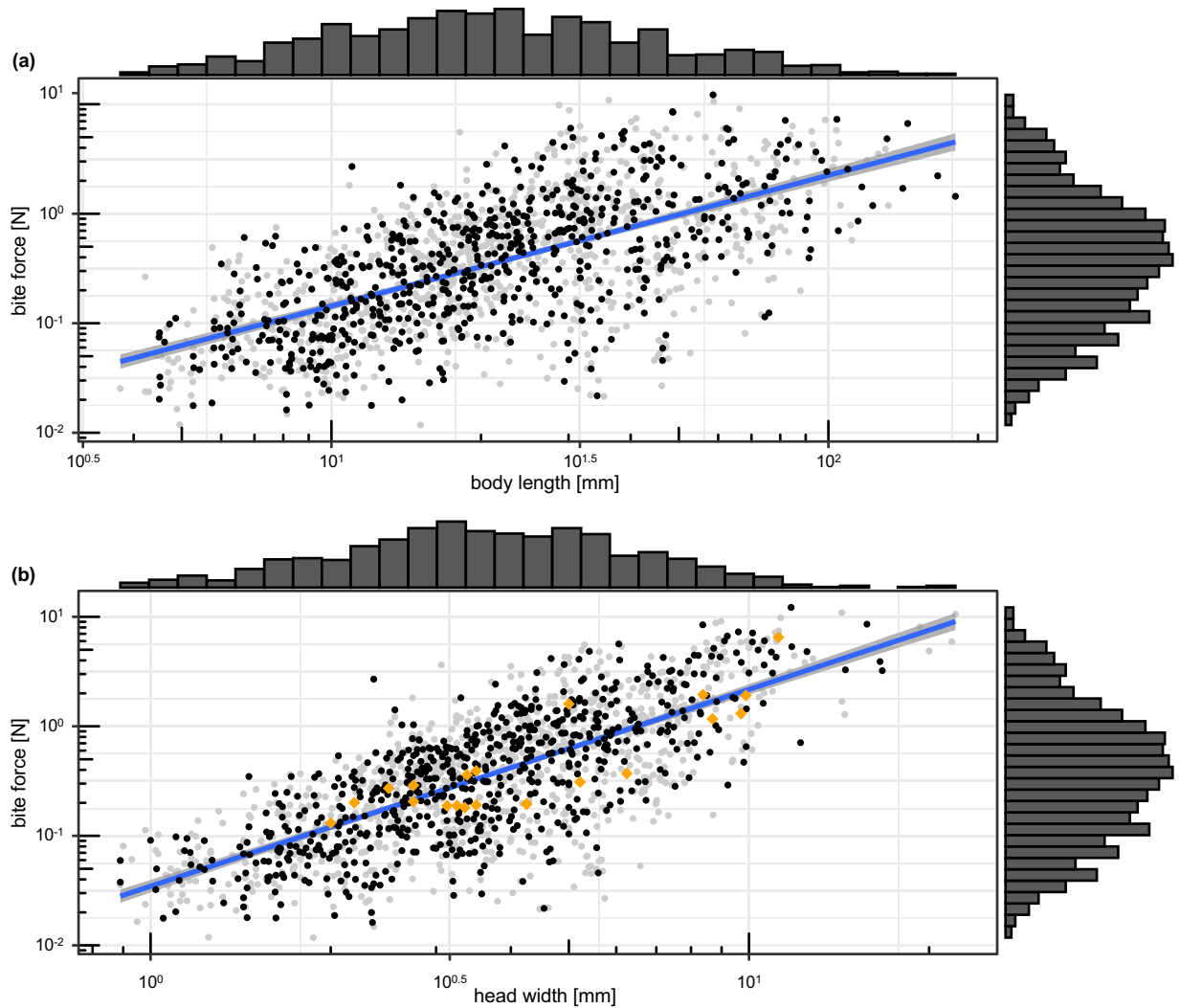
Fig. 2 Maximum bite force against body length (**a**) and head width (**b**). Grey dots show values of all measured specimens, black dots show geometric means per species. Marginal histograms at the x- and y-axes demonstrate mean size and mean bite force distribution per specimen, respectively. Regression lines and coefficients refer to log10-linear models of species-wise bite force against body length (**a**) or head width (**b**). Orange diamonds in (**b**) show bite force measurements available in previous literature. All axes are log10-transformed.

mechanics of the measurement system. Supplementary Table 1 shows all measurement settings, taxonomic classifications and information about which correction procedures have been performed on which measurements.

Maximum force value extraction for specimens and species. To extract maximum force values of each specimen and each species and calculate the standard deviations of these values we used the function 'summarize_measurements()' of forceR and custom code, relying on the 'dplyr' v.1.1 package[37]. We then plotted the log10-transformed average maximum bite force per specimen (grey dots in Fig. 2) and per species (black dots) against the log10-transformed average body length (Fig. 2a) and head width (Fig. 2b) using 'ggplot2' v.3.4.2[38] and 'ggExtra' v.0.9[39]. Linear regressions through the log10-transformed species-wise data showed a significant positive relationships between body size and head width ($p < 0.001$) with explanatory values of $R^2 = 0.44$ and $R^2 = 0.56$ respectively. Due to the expected logarithmic releationship between size and bite force[40], means were calculated as geometric means. Calculations with the regular mean, however, yielded similar results ($p < 0.001$, $R^2 = 0.44$ and $R^2 = 0.56$; Supplementary Fig. 1). Following existing literature, we use the term "maximum bite force" for the force that was produced by the animals during our experiments.

Comparison to previous insect bite force measurements. Previous studies on insect bite forces covered maximum bite force values for 32 species[21–28,41]. To check if these measurements follow similar allometric slopes as our data, we extracted all available insect bite force data from the literature and added them to the scatterplot in Fig. 2b, excluding data on 12 ant species because head width was not reported[25–27] or force was produced by mandible kinematics, not muscles[41]. We then tested if our data and the literature data differ in their allometric slopes by comparing a linear model with the null hypothesis of different slopes (log10(bite.force)~ log10(head.
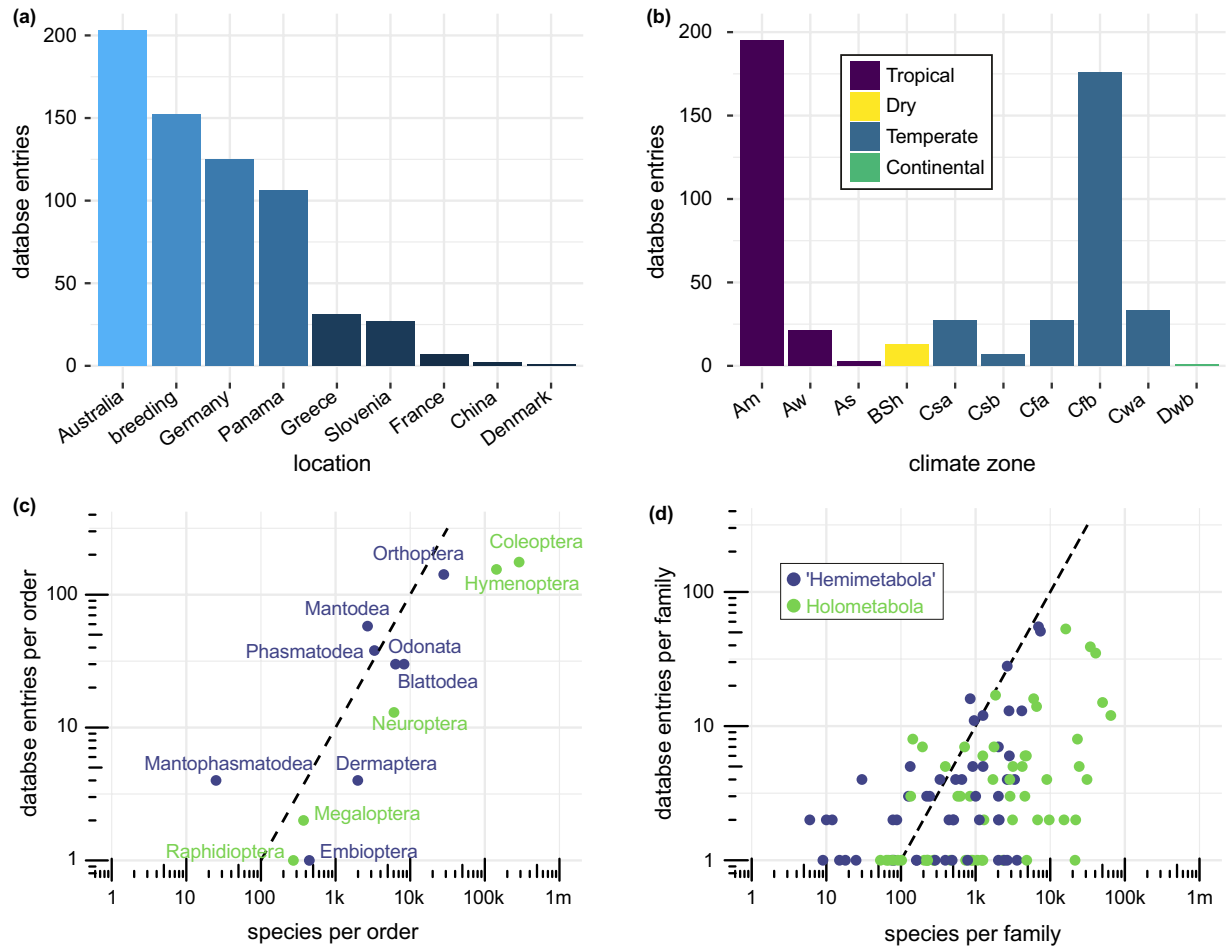
Fig. 3 Geographical and phylogenetic coverage of the bite force database. (**a**) Species entries per collection location (country or breeding). (**b**) Species entries per Köppen–Geiger climate zones[42–44] with specimens sourced from breeding cultures excluded. (**c**) Ratio of database entries compared to species estimated in all insect orders present in the database. (**d**) Ratio of database entries compared to species estimated in all insect families present in the database. The dashed lines in (c,d) mark a ratio of 1 data base entry per 100 estimated species. Abbreviations: **Am**: tropical monsoon; **Aw**: tropical savanna with dry-winter characteristics; **As**: tropical savanna with dry-summer characteristics; **BSh**: semi-arid (steppe) hot; **Csa**: mediterranean hot summer; **Csb**: mediterranean warm/cool summer; **Cfa**: humid subtropical; **Cfb**: oceanic; **Cwa**: dry-winter humid subtropical; **Dwb**: warm summer continental.

width) * source) versus a linear model with the null hypothesis of common slopes (log10(bite.force) ~ log10(-head.width) + source). Both model fits were compared with an ANOVA to find out if they differ significantly.

Assessment of geographical coverage.   Climate zone data (Köppen–Geiger classification system[42–44]) was gathered for each species based on the GPS coordinates of its collection localities (Supplementary Table 1) with the function 'LookupCZ()' of the R package 'kgc' v.1.0.0.2[45]. Percentages of species in the database for each country and climate zone were calculated.

Assessment of phylogenetic coverage.   To assess the phylogenetic coverage of the bite force database we compared the number of species with database entries to the number of species listed by the Open Tree of Life[46], accessed on 2022/02/05 with the function 'tol_node_info()' of the package 'rotl' v.3.0.14[47]. Comparisons were carried out for all insect orders and families that are present in the bite force database.

Data Records

All raw measurements and the cleaned data form the database at Zenodo[48]. All data files are available in comma-separated format as single files and in a combined long format converted to a 200 Hz sampling rate. Additionally, the database contains PDF plots and log files created during the conversion of the raw data to the final database. Supplementary Table 1 is also stored in the same repository.

Technical Validation

Visual inspection of the scatter plot of bite force against head width (black dots in Fig. 2b) and all literature data points (orange diamonds) revealed that the literature data lies close to the regression through all data points of our database. This impression is corroborated by the comparison of the allometric slopes of the insect bite force database and the literature data, which yielded no statistically significant difference (ANOVA: $F = 0.107$, $p = 0.74$).

Geographical assessment of the collected animals showed that most species of the insect bite force database were collected in Australia (31.0%), Germany (19.1%), and Panama (16.2%). 23.2% of the species were obtained from breeding cultures. The remaining 10.4% of the species were collected in Greece, Slovenia, France, China, and Denmark. Climate region assessment revealed that most species were collected in temperate (53.7%) and tropical (43.5%) regions. 2.8% came from dry and continental regions combined (Fig. 3b). We did not consider the original geographic distribution of those species obtained from breeding cultures.

A total of 13 biting-chewing insect orders are present in the database (Fig. 3d). We could not obtain live animals from the orders Zoraptera and Grylloblattodea. Bite force measurements of the few species of Plecoptera, Mecoptera, and Trichoptera that were available failed because no voluntary biting could be elicited in these specimens. We did not attempt measuring available representatives of Psocoptera and the biting-chewing "mandibulate archaic moths" (Lepidoptera: Micropterigoidea) due to their minute size. The assessment of phylogenetic coverage of the orders and families showed that most families are represented by less than one species entry per 100 estimated species (Fig. 3d,[46]). While orders were sampled in proportion to their taxonomic diversity (Fig. 3c), we were only able to measure at least 1% of the described species in Mantophasmatodea, Phasmatodea and Mantodea (dots left of dashed line in Fig. 3c). Accordingly, bite forces of only a fraction of all insect species were measured so far. Nevertheless, the database exceeds all previous studies combined in species numbers (20-fold in insects, 3.5-fold in amniotes), marking just the beginning of research on this performance trait in the most species-rich metazoan clade.

Usage Notes

The forceR package[31] was used to create the insect bite force database, which contains cleaned measurement time series and maximum bite forces of insects. The same package may be used to expand the scarce knowledge on insect bite forces by tackling questions regarding the evolution of bite lengths, frequencies, and bite curve shapes by semi-automatically extracting individual bite curves from these measurements. Additionally, the maximum bite force values presented in Supplementary Table 1 can be used for a wide range of in-depth studies on the morphological and ecological predictors and macroevolution of this important performance trait in the megadiverse insects.

Code availability

The R code to convert the raw measurements into the final database and to create all tables and figures used in this publication can be found at GitHub (https://github.com/Peter-T-Ruehr/InsectBiteForceDatabase) and Zenodo[49].

References

1. Aguirre, L. F., Anthony, H., van Damme, R. & Matthysen, E. Ecomorphological analysis of trophic niche partitioning in a tropical savannah bat community. *Proc. R. Soc. Lond. B Biol. Sci.* **269**, 1271–1278 (2002).
2. Huyghe, K., Vanhooydonck, B., Scheers, H., Molina-Borja, M. & Van Damme, R. Morphology, performance and fighting capacity in male lizards, *Gallotia galloti*. *Funct. Ecol.* **19**, 800–807 (2005).
3. Lappin, A. K. & Husak, J. F. Weapon performance, not size, determines mating success and potential reproductive output in the collared lizard (*Crotaphytus collaris*). *Am. Nat.* **166**, 426–436 (2005).
4. Husak, J. F., Lappin, A. K., Fox, S. F. & Lemos-Espinal, J. A. Bite-Force Performance Predicts Dominance in Male Venerable Collared Lizards (*Crotaphytus antiquus*). *Copeia* **2006**, 301–306 (2006).
5. Meyers, J. J., Nishikawa, K. C. & Herrel, A. The evolution of bite force in horned lizards: the influence of dietary specialization. *J. Anat.* **232**, 214–226 (2018).
6. Huber, D. R., Eason, T. G., Hueter, R. E. & Motta, P. J. Analysis of the bite force and mechanical design of the feeding mechanism of the durophagous horn shark *Heterodontus francisci*. *J. Exp. Biol.* **208**, 3553–3571 (2005).
7. Grubich, J. R., Huskey, S., Crofts, S., Orti, G. & Porto, J. Mega-Bites: Extreme jaw forces of living and extinct piranhas (Serrasalmidae). *Sci. Rep.* **2**, 1009 (2012).
8. Erickson, G. M. *et al*. Insights into the Ecology and Evolutionary Success of Crocodilians Revealed through Bite-Force and Tooth-Pressure Experimentation. *PLOS ONE* **7**, e31781 (2012).
9. Herrel, A., Podos, J., Huber, S. K. & Hendry, A. P. Evolution of bite force in Darwin's finches: a key role for head width. *J. Evol. Biol.* **18**, 669–675 (2005).
10. Herrel, A., O'Reilly, J. C. & Richmond, A. M. Evolution of bite performance in turtles. *J. Evol. Biol.* **15**, 1083–1094 (2002).
11. Herrel, A., Grauw, E. D. & Lemos-Espinal, J. A. Head shape and bite performance in xenosaurid lizards. *J. Exp. Zool.* **290**, 101–107 (2001).
12. Jones, M. E. H. *et al*. Reproductive phenotype predicts adult bite-force performance in sex-reversed dragons (*Pogona vitticeps*). *J. Exp. Zool. Part Ecol. Integr. Physiol.* **333**, 252–263 (2020).
13. Lappin, A. K. *et al*. Bite force in the horned frog (*Ceratophrys cranwelli*) with implications for extinct giant frogs. *Sci. Rep.* **7**, 11963 (2017).
14. Thomason, J. J., Russell, A. P. & Morgeli, M. Forces of biting, body size, and masticatory muscle tension in the opossum *Didelphis virginiana*. *Can. J. Zool.* **68**, 318–324 (1990).
15. Wroe, S., Colin, M. & Jeffrey, T. Bite club: comparative bite force in big biting mammals and the prediction of predatory behaviour in fossil taxa. *Proc. R. Soc. B Biol. Sci.* **272**, 619–625 (2005).
16. Christiansen, P. & Wroe, S. Bite Forces and Evolutionary Adaptations to Feeding Ecology in Carnivores. *Ecology* **88**, 347–358 (2007).
17. Santana, S. E. & Dumont, E. R. Connecting behaviour and performance: the evolution of biting behaviour and bite performance in bats. *J. Evol. Biol.* **22**, 2131–2145 (2009).

18. Sakamoto, M., Lloyd, G. T. & Benton, M. J. Phylogenetically structured variance in felid bite force: the role of phylogeny in the evolution of biting performance. *J. Evol. Biol.* **23**, 463–478 (2010).
19. Labandeira, C. C. Insect mouthparts: Ascertaining the paleobiology of insect feeding strategies. *Annu. Rev. Ecol. Syst.* **28**, 153–193 (1997).
20. Zhang, Z.-Q. Animal Biodiversity: An Outline of Higher-Level Classification and Survey of Taxonomic Richness. *Zootaxa* **3148**, 1–237 (2011).
21. David, S., Funken, J., Potthast, W. & Blanke, A. Musculoskeletal modelling of the dragonfly mandible system as an aid to understanding the role of single muscles in an evolutionary context. *J. Exp. Biol.* **219**, 1041–1049 (2016).
22. David, S., Funken, J., Potthast, W. & Blanke, A. Musculoskeletal modelling under an evolutionary perspective: deciphering the role of single muscle regions in closely related insects. *J. R. Soc. Interface* **13**, 20160675 (2016).
23. Weihmann, T., Reinhardt, L., Weißing, K., Siebert, T. & Wipfler, B. Fast and Powerful: Biomechanics and Bite Forces of the Mandibles in the American Cockroach *Periplaneta americana*. *PLoS ONE* **10**, e0141226 (2015).
24. Patek, S. N., Baio, J. E., Fisher, B. L. & Suarez, A. V. Multifunctionality and mechanical origins: Ballistic jaw propulsion in trap-jaw ants. *Proc. Natl. Acad. Sci.* **103**, 12787–12792 (2006).
25. Huang, M. H. Extreme Worker Polymorphism in the Big-headed *Pheidole* Ants. (The University of Arizona, 2012).
26. Püffel, F., Roces, F. & Labonte, D. Strong positive allometry of bite force in leaf-cutter ants increases the range of cuttable plant tissues. *J. Exp. Biol.* **226**, jeb245140 (2023).
27. Püffel, F., Johnston, R. & Labonte, D. A biomechanical model for the relation between bite force and mandibular opening angle in arthropods. *R. Soc. Open Sci.* **10**, 221066 (2023).
28. Wheater, C. P. & Evans, M. E. G. The mandibular forces and pressures of some predacious Coleoptera. *J. Insect Physiol.* **35**, 815–820 (1989).
29. Goyens, J., Dirckx, J., Dierick, M., Hoorebeke, L. V. & Aerts, P. Biomechanical determinants of bite force dimorphism in *Cyclommatus metallifer* stag beetles. *J. Exp. Biol.* **217**, 1065–1071 (2014).
30. Grimaldi, D. A. & Engel, M. S. *Evolution of the Insects*. (Cambridge University Press, 2005).
31. Rühr, P. T. & Blanke, A. forceX and forceR: A mobile setup and r package to measure and analyse a wide range of animal closing forces. *Methods Ecol. Evol.* **13**, 1938–1948 (2022).
32. Herrel, A., Spithoven, L., van Damme, R. & de Vree, F. Sexual dimorphism of head size in *Gallotia galloti*: testing the niche divergence hypothesis by functional analyses. *Funct. Ecol.* **13**, 289–297 (1999).
33. Gomes, V., Herrel, A., Carretero, M. A. & Kaliontzopoulou, A. New Insights into Bite Performance: Morphological Trade-Offs Underlying the Duration and Magnitude of Bite Force. *Physiol. Biochem. Zool.* **93**, 175–184 (2020).
34. Lappin, A. K. & Jones, M. E. H. Reliable quantification of bite-force performance requires use of appropriate biting substrate and standardization of bite out-lever. *J. Exp. Biol.* jeb.106385 https://doi.org/10.1242/jeb.106385 (2014).
35. R Core Team. R: A language and environment for statistical computing. R Foundation for Statistical Computing. (2022).
36. Blondel, E., Barde, J., Eglen, S., Calster, H. V. & Vanderhaeghe, F. zen4R: Interface to 'Zenodo' REST API. (2023).
37. Wickham, H. *et al.* dplyr: A Grammar of Data Manipulation. (2023).
38. Wickham, H. *et al.* ggplot2: Create Elegant Data Visualisations Using the Grammar of Graphics. (2021).
39. Attali, D. & Baker, C. ggExtra: Add Marginal Histograms to 'ggplot2', and More 'ggplot2' Enhancements. (2019).
40. Sakamoto, M., Ruta, M. & Venditti, C. Extreme and rapid bursts of functional adaptations shape bite force in amniotes. *Proc. R. Soc. B Biol. Sci.* **286**, 20181932 (2019).
41. Spagna, J. C. *et al.* Phylogeny, scaling, and the generation of extreme forces in trap-jaw ants. *J. Exp. Biol.* **211**, 2358–2368 (2008).
42. Köppen, W. Das geographische System der Klimate. in *Handbuch der Klimatologie* (ed. Geiger, R.) 5–44 (Borntraeger, 1936).
43. Rubel, F. & Kottek, M. Observed and projected climate shifts 1901–2100 depicted by world maps of the Köppen-Geiger climate classification. *Meteorol. Z.* 135–141 https://doi.org/10.1127/0941-2948/2010/0430 (2010).
44. Rubel, F., Brugger, K., Haslinger, K. & Auer, I. The climate of the European Alps: Shift of very high resolution Köppen-Geiger climate zones 1800–2100. *Meteorol. Z.* 115–125 https://doi.org/10.1127/metz/2016/0816 (2017).
45. Bryant, C., Wheeler, N. R., Rubel, F. & French, R. H. kgc: Koeppen-Geiger Climatic Zones. (2017).
46. Hinchliff, C. E. *et al.* Synthesis of phylogeny and taxonomy into a comprehensive tree of life. *Proc. Natl. Acad. Sci.* **112**, 12764–12769 (2015).
47. Michonneau, F., Brown, J. W. & Winter, D. J. rotl: an R package to interact with the Open Tree of Life data. *Methods Ecol. Evol.* **7**, 1476–1481 (2016).
48. Rühr, P. T., Edel, C., Frenzel, M. & Blanke, A. A bite force database of 654 insect species v.1.0.0. *Zenodo* https://doi.org/10.5281/zenodo.8183211 (2022).
49. Rühr, P. T. R. Code for the creation of the insect bite force database. *Zenodo* https://doi.org/10.5281/zenodo.8183406 (2023).
50. Snodgrass, R. E. Facts and theories concerning the insect head. *Smithson. Misc. Collect.* **142**, 1–61 (1960).
51. Snodgrass, R. E. *Insects, their ways and means of living*. (Smithsonian Institution, 1930).

Acknowledgements

Author contributions
P.T.R. wrote all code, prepared the figures, lead the dataset creation and drafted the manuscript. PTR and AB conceived the study and refined the manuscript. CE, MF and AB contributed to the dataset creation. All authors reviewed the manuscript and gave final approval for publication.

Funding
Open Access funding enabled and organized by Projekt DEAL.

Competing interests
The authors declare no competing interests.

Additional information
Supplementary information The online version contains supplementary material available at https://doi.org/10.1038/s41597-023-02731-w.

Correspondence and requests for materials should be addressed to P.T.R.

Reprints and permissions information is available at www.nature.com/reprints.

Publisher's note Springer Nature remains neutral with regard to jurisdictional claims in published maps and institutional affiliations.